JOURNAL OF GEOPHYSICAL RESEARCH, VOL. 113, C06028, doi:10.1029/2007JC004236, 2008

Relation between the wind stress curl in the North Atlantic and the Atlantic inflow to the Nordic Seas

A. B. Sandø[1,2] and T. Furevik[2,3]

Received 21 March 2007; revised 1 April 2008; accepted 16 April 2008; published 27 June 2008.

[1] In this study an isopycnic coordinate ocean model has been used to investigate the relationships between the North Atlantic wind stress curl (WSC) and the inflow of Atlantic water to the Nordic Seas. For the period 1995–2001, there is a maximum in the correlation between the zonally averaged WSC at 55°N and the inflow with a 15-month time lag, capturing a relation already found in observational data. In the model this relation is linked to the mixing along the western flank of the Rockall Bank (56°N, 15°W). For the period 1995–2001 the atmospheric forcing in the northeastern North Atlantic is relatively weak, and the depth of the mixed layer is shallower than the sill depths of the Greenland-Scotland Ridge (GSR). Slowly moving, baroclinic disturbances caused by anomalies in the wind forcing will then be transmitted into the Nordic Seas where they are recorded as anomalous volume transports in the Norwegian Atlantic Current. In contrast, for the pentad prior to this period the atmospheric forcing is much more intense, and generates mixing well below sill depths of the GSR for all winters. Baroclinic disturbances forced by variations in the atmospheric forcing will then tend to follow f/H contours that do not enter the Nordic Seas, and the 15-month lagged relations between the wind and the volume transports will vanish. Recent observational data support this view.

Citation: Sandø, A. B., and T. Furevik (2008), Relation between the wind stress curl in the North Atlantic and the Atlantic inflow to the Nordic Seas, *J. Geophys. Res.*, *113*, C06028, doi:10.1029/2007JC004236.

1. Introduction

[2] The inflow of warm and saline Atlantic water into the Nordic Seas is of significant importance to the regional ocean climate, as well as for the biomass production and fish distribution within the Nordic Seas [*Hansen and Østerhus*, 2000; *Lehodey et al.*, 2006]. Much effort has therefore been spent to explore the potential predictability of the system, either based on observed time lags between hydrographic sections along the Atlantic water pathways [*Helland-Hansen and Nansen*, 1909; *Furevik*, 2001], on observed time lags between atmospheric forcing and observed currents [*Orvik and Skagseth*, 2003], or on ensemble techniques using ocean or coupled atmosphere–ocean models [*Collins et al.*, 2006].

[3] In order to forecast the properties and strength of the Atlantic inflow, and thus its impacts on the hydrographical and ecological conditions of the Nordic Seas, the mechanisms behind the variability and in particular the role of the atmospheric forcing should be known. A motivation for this study has been the findings of *Orvik and Skagseth* [2003], who reported a 15-month time lag between the averaged WSC at 55°N and the mass transports in the eastern part of the Svinøy section (Figure 1), capturing the extension of the North Atlantic Current feeding the Barents Sea and Arctic Ocean with warm, saline Atlantic water. According to *Orvik and Skagseth* [2003] the 15-month time lag is caused by forced baroclinic Rossby waves associated with anomalous Ekman pumping along the path of the North Atlantic Current. Interaction with topography along the Irish-Scottish shelf then transfers energy from the baroclinic waves to the barotropic shelf edge current, eventually being recorded as low-frequency anomalies in the Norwegian Atlantic Current at the Svinøy section.

[4] To further explore the mechanisms for the lagged responses to the WSC we will in this study focus on the slowly varying baroclinic processes south of the GSR. Key questions that will be addressed are: How are baroclinic fluctuations in mass transports initially generated in the North Atlantic? How do the baroclinic signals propagate across the GSR? How robust is the suggested link between WSC and the Atlantic inflow to the Nordic Seas? Is there a predictability in the system?

[5] The long quasi-permanent and still existing direct current measurements started in the mid 1990's both in the inflow branches (Nordic WOCE project) and in the Norwegian Atlantic Slope Current [*Østerhus et al.*, 2005; *Orvik et al.*, 2001]. The lack of observed current data prior to 1995 is therefore a limitation in studies of causes and effects related to volume transport variabilities. Our best approach is therefore to apply an Ocean General Circulation

[1] G. C. Rieber Climate Institute, Nansen Environmental and Remote Sensing Center, Bergen, Norway.
[2] Bjerknes Centre for Climate Research, Bergen, Norway.
[3] Geophysical Institute, University of Bergen, Bergen, Norway.

0148-0227/08/2007JC004236$09.00

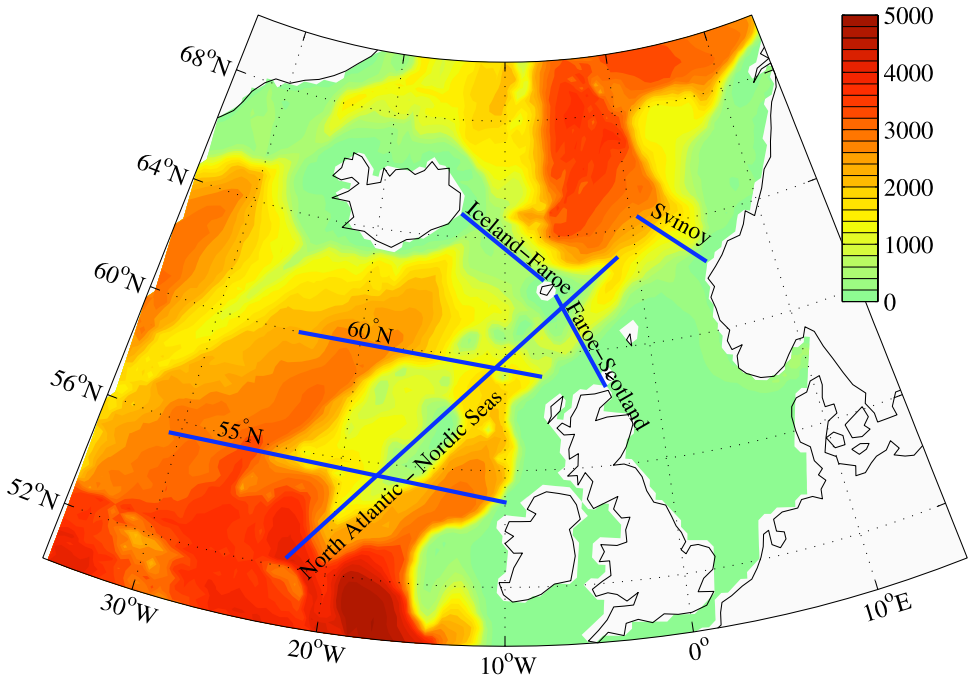

Figure 1. Model bathymetry and vertical sections where volume transports and Hovmöller diagrams are taken from.

Model (OGCM), which provides us with simulated hydrography and current data with relatively good coverage in space and time, given that the model reflects the reality. The model systems in general have undergone significant improvements over the last decades, and present OGCMs can often complement available ocean observations, and more important, be used as laboratories for assessing cause relationships for observed changes in the marine climate system [e.g., *Drange et al.*, 2005].

[6] The particular model system used for this study is presented in section 2. In section 3 we provide a brief description of the various analyses techniques used in this study, before results are shown in section 4. The implications of the various findings are discussed in section 5, before the paper is summarized and concluded in section 6.

2. Model Description

[7] For this study we are using a regional version of the Miami Isopycnic Coordinate Ocean Model (MICOM) [*Bleck et al.*, 1992], set up for the North Atlantic and the Nordic Seas from Cape Hatteras to the Fram Strait. Favorable comparisons between this state of the art model system and observations have previously been discussed by *Hátun et al.* [2005a, 2005b] and *Eldevik et al.* [2005]. Details about the regional model and its setup are given by *Sandø and Drange* [2006].

[8] The regional model is integrated for the period 1948–2005 using daily atmospheric forcing data from NCEP/NCAR [*Kistler et al.*, 2001]. Output data from a spin up of a global version of MICOM [*Furevik et al.*, 2002; *Nilsen et al.*, 2003; *Bentsen et al.*, 2004] has been used to initialize the model. The global model has a grid spacing of about 40 km over most of the North Atlantic whereas the nested model has about 20 km. Otherwise the grid distribution of the two model configurations remains the same. In the vertical, both model versions have 26 layers, where the uppermost is the thermodynamically active mixed layer while layers 2–26 are layers of constant density.

[9] The boundary conditions for the regional model are given from an integration with the global version forced by the same atmospheric forcing fields. For the regional model set up, daily NCEP/NCAR reanalysis fresh water, heat and momentum fluxes are used to force the system by applying the scheme of *Bentsen and Drange* [2000]: If the model sea surface state is close to the derived sea surface state from the NCEP/NCAR reanalysis data, the NCEP/NCAR fluxes are used without modification. If, however, there are significant differences between model and reanalysis sea surface states, the fluxes of momentum and heat are modified according to the scheme by *Fairall et al.* [1996].

[10] Mixed layer temperature and salinity fields are linearly relaxed toward the monthly mean climatological values of *Levitus et al.* [1994] and *Levitus and Boyer* [1994], respectively. The e-folding relaxation timescale is set to 30 days for a 50 m thick mixed layer. The timescale increases linearly when the mixed layer depth exceeds 50 m. This relaxation is sufficiently weak to allow anomalies to develop and persist for years to decades, as shown by *Hátun et al.* [2005b].

[11] The model is coupled to a sea-ice module consisting of the *Hibler* [1979] rheology, implemented by *Harder* [1996], and the thermodynamics of *Drange and Simonsen* [1996]. Realistic runoff is incorporated through the NCEP/NCAR reanalysis data and the TRIP database [*Oki and Sud*, 1998]. A further description of the model system is given by *Hátun et al.* [2005a, 2005b] and *Sandø and Drange* [2006].

[12] The model has been thoroughly evaluated in the area of discussion, both with respect to hydrography, but also the current systems in terms of the interplay between the

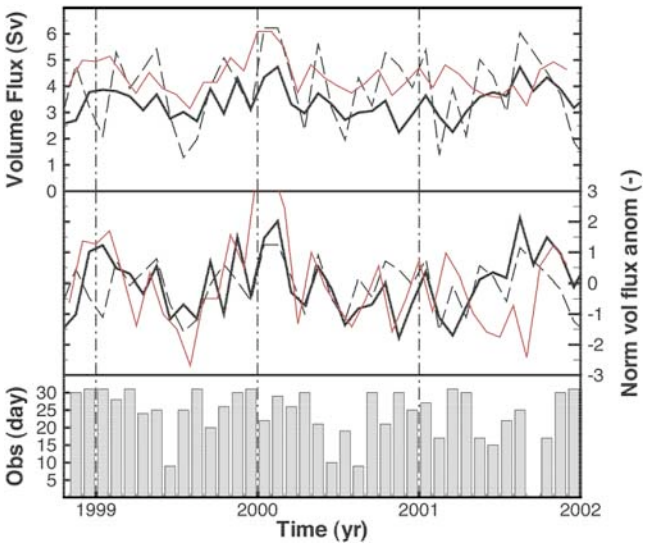

Figure 2. Observed and simulated northward volume transports through the Faroe-Scotland Channel. (top) Observed transport (Sv) based on current-meter measurements [*Østerhus et al.*, 2005] in dashed line, simulated regional (global) transport (Sv) in red (black) solid line. (middle) Corresponding volume flux anomalies, normalized with respect to the standard deviation of the respective time series. (bottom) Number of days per month when observations were made.

subpolar and subtropical gyres, and the current in between, namely the North Atlantic Current. *Hátun et al.* [2005a] found that the simulated long-term temperature variations in the Faroe-Shetland inflow waters closely resemble observations south of the ridge (Rockall Trough), north of the ridge (Svinøy section) and between (Faroe-Shetland Channel). [*Hátun et al.*, 2005b] show that simulated salinity variations of the three Atlantic inflow branches are accurately simulated, and that this is closely linked to the dynamics of the North Atlantic subpolar gyre circulation, and in particular the mixing of subpolar and subtropical waters in the Rockall area. This satisfactory simulation of the hydrography in combination with realistic atmospheric forcing in the area should result in a realistic mixed layer density, vertical mixing and mixed layer depth.

3. Methods

[13] The atmospheric forcing data and the model output will be explored to address the key questions given above. As the focus of this study is on low frequency variability, the annual cycle has been subtracted prior to all analyses by applying a 12-month running mean filter.

3.1. Communication Between Surface and Deep Ocean

[14] In order to identify possible upstream mechanisms responsible for the observed variations in the Norwegian Atlantic Current, different kinds of analyses will be performed either directly on thicknesses or depths of isopycnic layers, or on volume transports of Atlantic water through standard sections (Figure 1). The Atlantic water is here defined as water with salinities greater than 35.1 and densities in σ_0 units less than or equal to 27.38 (layers 1–11), as water denser than this only infrequently pass over the GSR in the model.

[15] The water mass contained within an isopycnic layer can vary with time owing to four processes: entrainment, detrainment, convective mixing, or diapycnal mixing. The first three processes are all related to corresponding changes in the mixed layer thickness, and to direct atmospheric forcing processes such as momentum, heat and freshwater fluxes. The fourth process is due to internal mixing between the isopycnic layers and is, in general, several orders of magnitude less efficient than the other processes.

[16] Redistribution of water masses within an isopycnic layer, and thus changes in the slopes of the interfaces between the isopycnic layers, are typically caused by wind forcing and subsequent Ekman transports and Ekman pumping. Divergence (convergence) in the Ekman transports forces positive (negative) Ekman pumping and a shallowing (deepening) of the interfaces.

3.2. Correlation Analysis Techniques

[17] Standard lag regression (slope in linear fits) are performed between the properties of the isopycnic layers and volume transports through key sections. The isopycnic layers focused on in this study are layers 11 and 12 with the corresponding densities in σ_0 values 27.38 and 27.52, respectively. These layers contain the densest Atlantic water that passes over the GSR.

[18] Covariability in the transports through the various sections are explored by lag correlation analysis. All given values are normalized according to

$$cor(k) = \frac{\Sigma x_{(n+k)} y_n}{\sqrt{\Sigma x_n^2 \Sigma y_n^2}},$$

where x and y are the two time series, k the lag (positive when y leads), and we sum over all months n. The autocorrelation at zero lag is exactly 1.

[19] The significance levels for the correlation results are estimated using the bootstrap algorithm described by *Zoubir and Boashash* [1998]. For each of the two time series we first make 10000 permutations, where each permutation has the same mean, standard deviations and lag one correlation (memory) as the original time series. Then the correlations are calculated for each of the 10000 pairs of artificial time series, and finally the 95 and 99% confidence intervals are estimated as the corresponding percentiles of the distribution of the results.

4. Results

[20] As reported in previous studies, the model shows a reasonable agreement with observed hydrography and flow field in the North Atlantic–Nordic Seas area [*Hátun et al.*, 2005a, 2005b; *Eldevik et al.*, 2005; *Drange et al.*, 2005; *Mauritzen et al.*, 2006]. An example of the performance is given in Figure 2, showing a comparison between observed and simulated northward volume transport through the Faroe-Shetland Channel. Both the regional model used in this study, and the global model used to force the regional model, do capture most of the variations seen in the observational data. The regional model has a mean transport

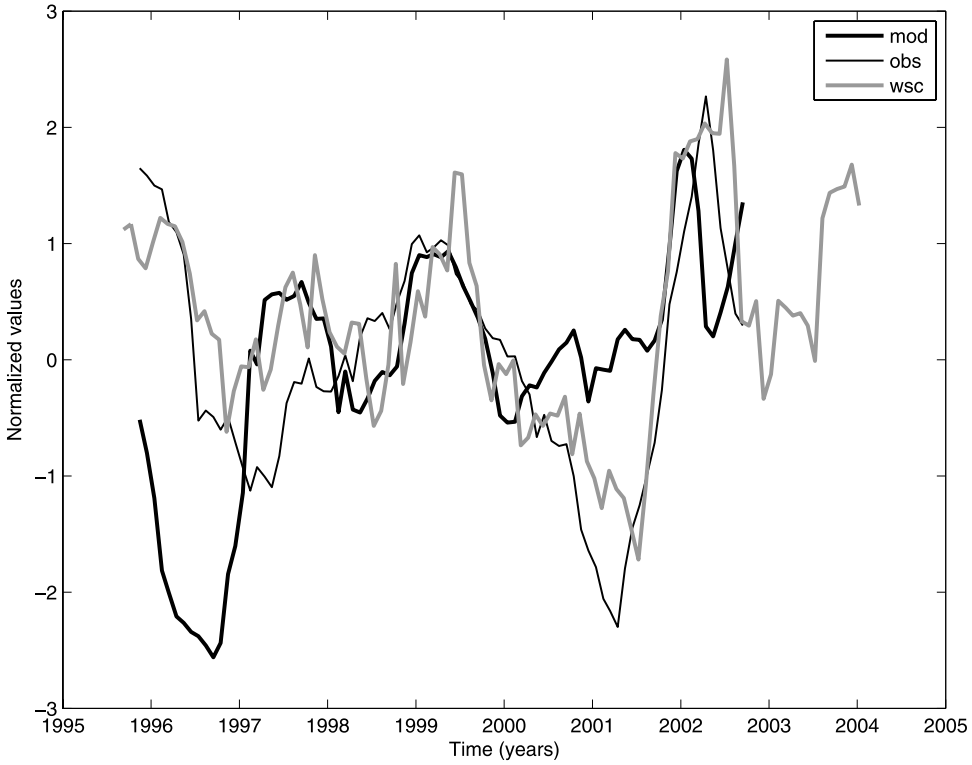

Figure 3. Time series representing the variability of the Norwegian Atlantic Slope Current, the zonally integrated WSC from *Orvik and Skagseth* [2003], and the variability of the modeled current. An offset is subtracted from the WSC time to illustrate the maximum correlation at 15 months time lag.

that is 1 Sv higher than the global model, and is closer to the observed values reported by *Østerhus et al.* [2005].

4.1. Wind Stress Curl and Oceanic Volume Transports

[21] The results from *Orvik and Skagseth* [2003] were based on measurements from a single mooring location for the period 1995–2003. The modeled position of the Norwegian Atlantic Current in the Svinøy section is not as confined over the steep slope (200–900 m) as the observations indicate [*Orvik et al.*, 2001]. A wider section is therefore used to capture the northward flow of Atlantic water in the model. In Figure 3 the observed and modeled volume transport estimates are plotted together with the WSC at 55°N for the period in common. The WSC time series is displaced 15 months to illustrate the maximum correlation at this time lag. The model does not perfectly give the same volume transports as those estimated by *Orvik and Skagseth* [2003], both due to model deficiencies and probably also due to uncertainties in the observed volume transport estimates. The WSC and the modeled transports show the same variability even though the amplitudes differ in a couple of periods (in 1996 and 2001). Periodically, the fit between the modeled transports and the WSC is better than between the observed transports and the WSC (in 1997 and 2000). Nevertheless, a perfect match between the WSC and the volume transports, either modeled or observed, should not be expected. Potential model deficiencies, the use of a single mooring location, and the influence of other physical processes than the WSC on the volume transports, will all tend to disturb such a relation.

[22] As a result of the discrepancies pointed out, the relationships between the North Atlantic WSC and the Svinøy transports are only partly reproduced (Figure 4). The model does show, however, a maximum in the covariability between the WSC at 55°N and the volume transports at Svinøy around 15 months later, the same latitude and time lag as pointed out by *Orvik and Skagseth* [2003]. Even though the period when this relation is valid is slightly shorter than in the observations, it suggests that the model can be used to study the causal relationships behind the *Orvik and Skagseth* [2003] results.

[23] On the basis of observations, the majority of the flow monitored in the eastern part of the Svinøy section, enters through the Faroe-Scotland (FS) section [*Orvik and Niiler*, 2002], although there is some leakage from the branch entering through the Iceland-Faroe (IF) section due to recirculation east of the Faroes [*Østerhus et al.*, 2005]. In order to identify where the atmospherically forced baroclinic disturbances pass over the GSR in the model, the correlation analysis against the WSC are repeated for the volume transports in the FS and IF sections. It turns out that the IF transports reveal a correlation pattern with the WSC at 55°N (Figure 5) that closely resembles the corresponding correlation with Svinøy. This is in contrast to the FS transports that did not reproduce the found correlations (not shown). The analysis has in the following therefore been concentrated on the IF inflow branch.

4.2. Upstream Variations in the Baroclinic Structure

[24] The atmosphere is forcing the ocean through fluxes of momentum, heat and freshwater (for a review, see

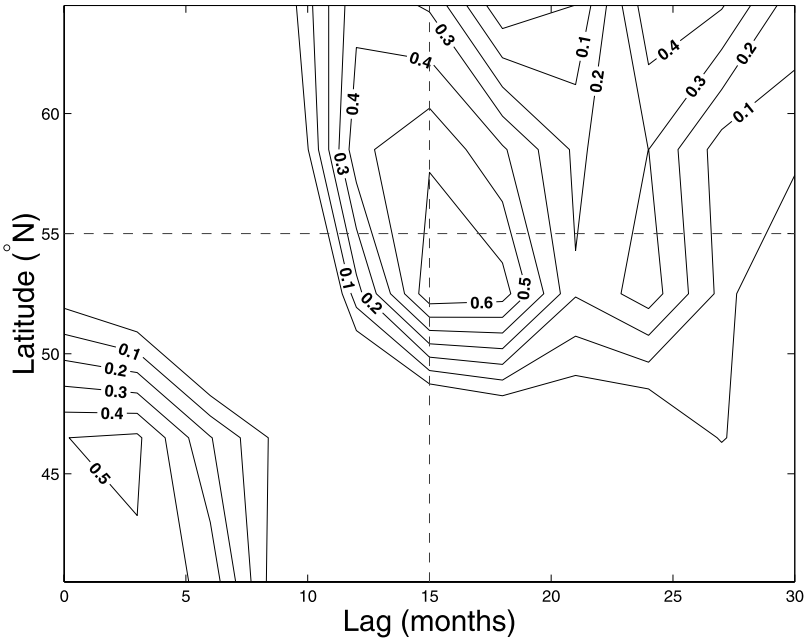

Figure 4. Correlation between zonally averaged (40°W–10°E) WSC and volume transports at Svinøy at different time lags and latitudes (1995–2001). Dashed lines mark the 15-month time lag and the 55°N latitude.

Furevik and Nilsen [2005]). These fluxes can change the internal density and pressure distribution in the fluid, resulting in slowly propagating baroclinic waves and adjustment processes [*Gill*, 1982]. For the isopycnic ocean model in use, Ekman pumping associated with momentum fluxes, or convection associated with buoyancy forcing, will be manifested in the depth and thickness of the isopycnal layers.

[25] In Figure 6 the thickness of layer 11 is regressed upon the volume transports through the IF section from 1995 through 2001. On the basis of this analysis, an increase of 1 Sv in the inflow is preceded by an increase of more than 300 m in the thickness of layer 11 at the western flank of the Rockall Bank one and a half years earlier. This signal is gradually moving north and west, and at the time of enhanced inflow through the IF section, the

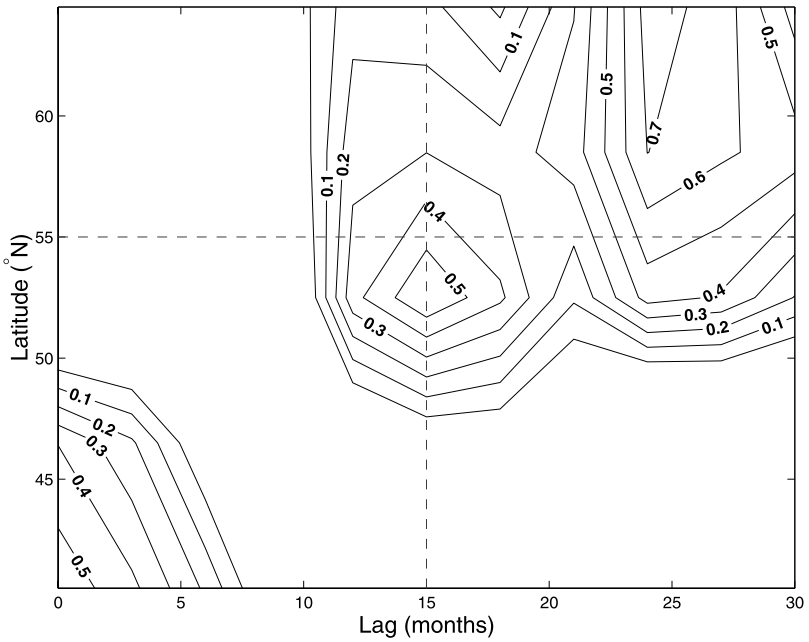

Figure 5. Correlation between zonally averaged (40°W–10°E) WSC and volume transports at IF at different time lags and latitudes (1995–2001). Dashed lines mark the 15-month time lag and the 55°N latitude.

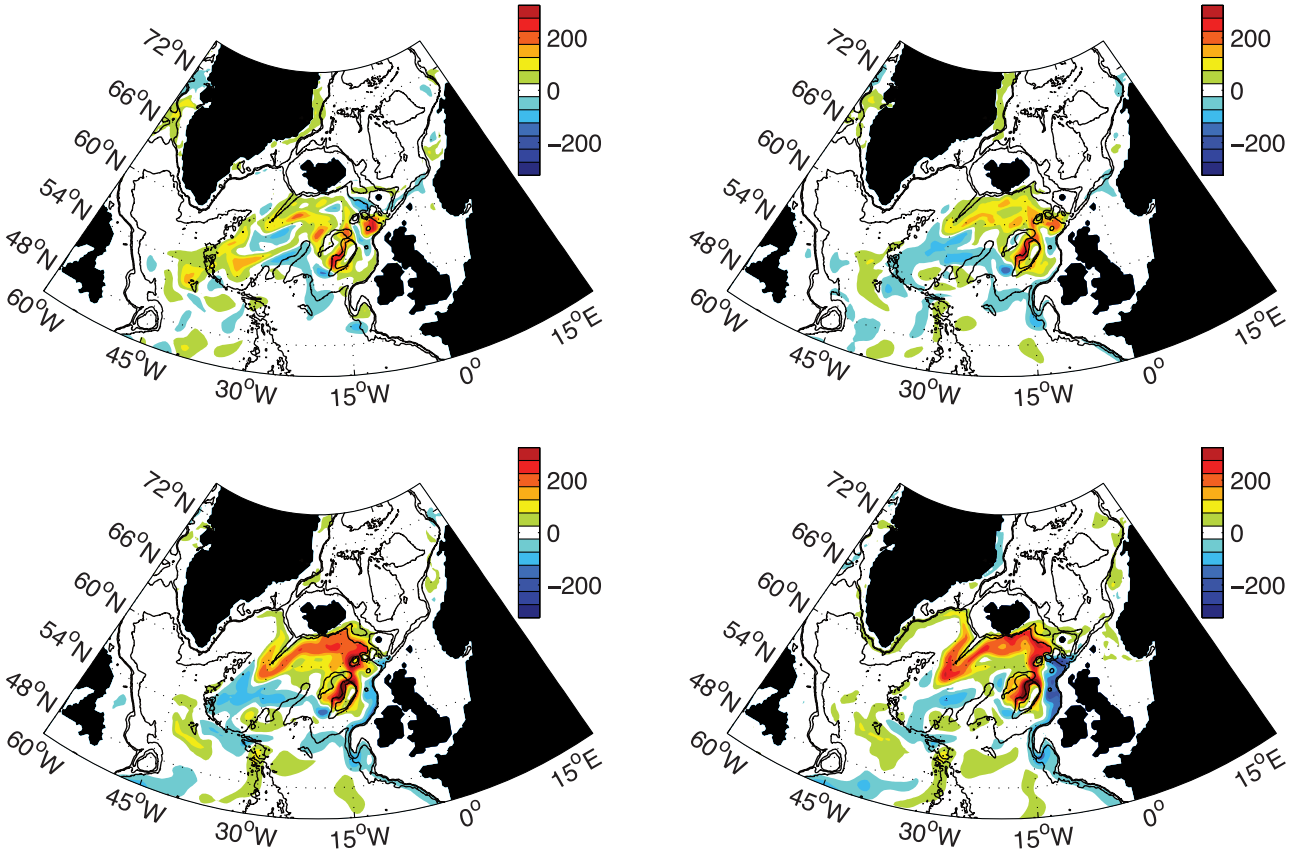

Figure 6. Regression between the volume transports in the IF opening and the thickness of layer 11 with time lags of (top left) 21, (top right) 14, (bottom left) 7, and (bottom right) 0 months (1995–2001). Black contour corresponds to 500, 1000, and 3000 m depth.

region of a thicker layer 11 is extending from south of the IF inflow and west to the Irminger Basin. Both advection of anomalous water properties and slowly moving baroclinic shelf waves may play active roles here.

[26] The northward flow of Atlantic water (defined as layers 1–11, $\sigma_0 \leq 27.38$) has further been calculated through a 55°N and a 60°N section (Figure 1), and correlated with the transports through the IF and FS sections (Figure 7). The analysis shows correlations exceeding the 95% confidence threshold for both IF and FS sections and for both periods, but only the IF section and the 1995–2001 period shows correlation exceeding the 99% confidence interval. The IF section is seen to lag the 55°N and 60°N sections with 10–20 months, indicating slowly moving baroclinic disturbances.

4.3. Extension of Analysis Prior to Observations

[27] With the model at hand, we may ask whether the lagged relations between WSC and current variability are valid also for periods prior to the 1995–2003 period studied by *Orvik and Skagseth* [2003]. To test this we have performed the same analysis on the 1990–1995 period. First correlating the Svinøy transport with the North Atlantic WSC (Figure 8), it is evident that the correlation between the transports and the WSC at 55°N 15 months prior is no longer present. Instead there is a significant correlation at zero lag, indicating that this period is more dominated by forcing on barotropic timescales. Furthermore, regression between the layer 11 thickness and the IF inflow differs completely from the 1995–2001 period (Figure 6), as no systematic pattern emerges (Figure 9). There is, however, an indication of a signal developing in the Rockall Trough only a couple of months prior to the inflow at the GSR.

[28] Finally, a comparison between the transports through the 60°N section and the IF and FS inflows (Figure 10), again emphasizes the difference between the two periods. The significant correlations between the IF inflow and the section to the south is no longer present, instead there is an enhanced (although not statistically significant) correlation between the 60°N and the FS sections at zero lag, indicating that barotropic processes are dominating these years.

4.4. Atmospheric Forcing, Mixed Layer Density, and Internal Density Structure

[29] The atmospheric circulation variability over the North Atlantic is dominated by the number and strengths of storms passing by each winter. From the winter ending in 1995 to the winter ending in 1996, there was a large decrease in the storm activity, manifested for instance by a record drop in the commonly used North Atlantic Oscillation index [e.g., *Hurrell et al.*, 2001]. If we once more consider the effects of the winds, specifically the time series of the WSC, wind stress and the heat loss in a rectangular area (20°W–10°W, 54°N–56°N) over the Rockall Bank (Figure 11), it can be seen that the atmospheric forcing became considerably reduced after 1995. The combined

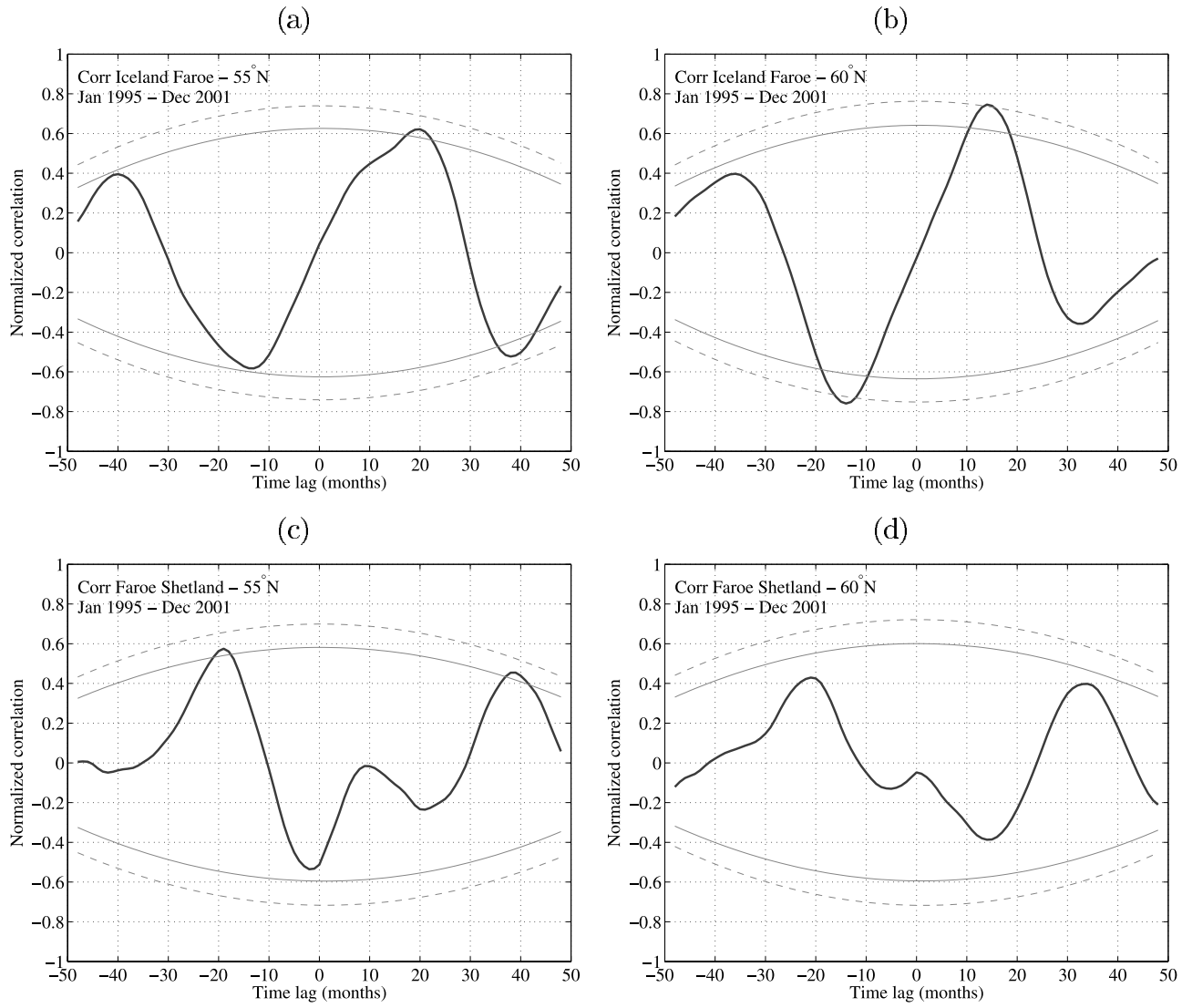

Figure 7. Correlation (a) between northward transports in the IF section 1995–2001 and the 55°N section, (b) between IF and the 60°N section, (c) between the FS section and the 55°N section, and (d) between the FS section 1995–2001 and the 60°N section. Thin solid and dashed lines indicate, respectively, the 95 and 99% confidence intervals, estimated using a bootstrap algorithm with 10,000 permutations. Positive lag means that IF or FS is lagging the other sections.

effect of a weaker WSC, which through Ekman pumping causes a doming of the isopycnals, less wind mixing and thus reduced up-mixing of dense subsurface water, and less heat loss, will all lead to reduced mixed layer density.

[30] Changes in the mixed-layer density caused by atmospheric forcing will be most efficiently communicated to the interior layer with the corresponding density through entrainment and convection processes. In Figure 12 a Hovmöller diagram for the mixed layer density in a section running from the North Atlantic and into the Nordic Seas is shown (Figure 1). Strong variability in mixed layer density is found over the Rockall Bank (57°N), and from 1995 to 1996 the annual maximum mixed layer density was reduced by more than $0.1\sigma_0$ units from 27.54 to 27.42. The reduced density leads to shallower mixing, as only the isopycnals that outcrop during winter will receive new water in the restratification (detrainment) process the following spring. For the particular mixed layer density change, this means that mixing could only reach layer 11 in 1996 compared to layer 12 in 1995. The mixed layer density also affects the mixed layer thickness as shown in Figure 13. The difference between the two periods (1990–1995 and 1996–2001) are shown by the reduced mixed layer depths at the western flank of the Rockall Bank in the second period.

[31] Enhanced topographic mixing over shallow banks and steep bottom slopes makes the upper isopycnals to some extent follow the underlying topography. Shallow areas like the Rockall Bank and along the Irish shelf may therefore be more sensitive to atmospheric forcing than the deeper parts of the ocean basin. An example of this is shown in Figure 14, where strong atmospheric forcing and deep mixing in 1990–1995 made layer 12 very thick in the

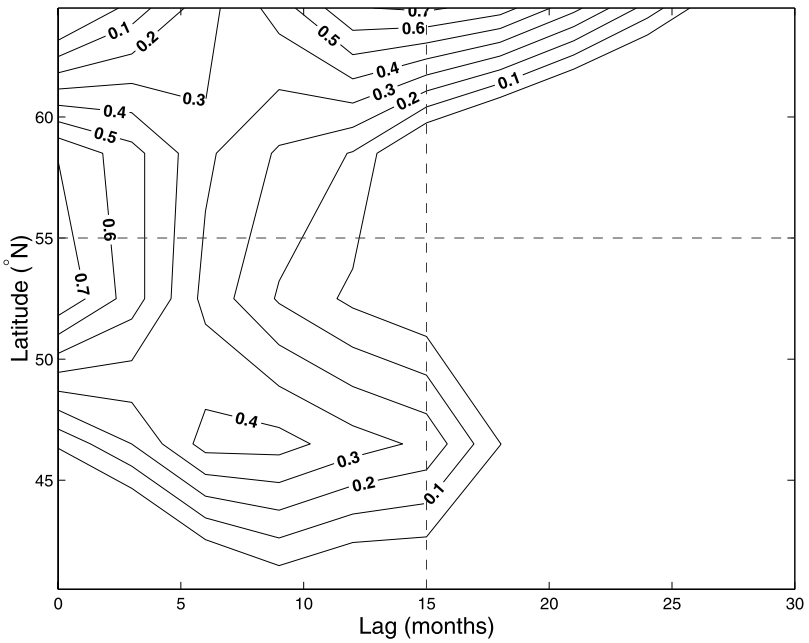

Figure 8. Correlation between zonally averaged (40°W–10°E) WSC and volume transports at Svinøy at different time lags and latitudes (1990–1995). Dashed lines indicate the local maximum where the WSC at 55°N leads the inflow by 15 months in the period from 1995 to 2001.

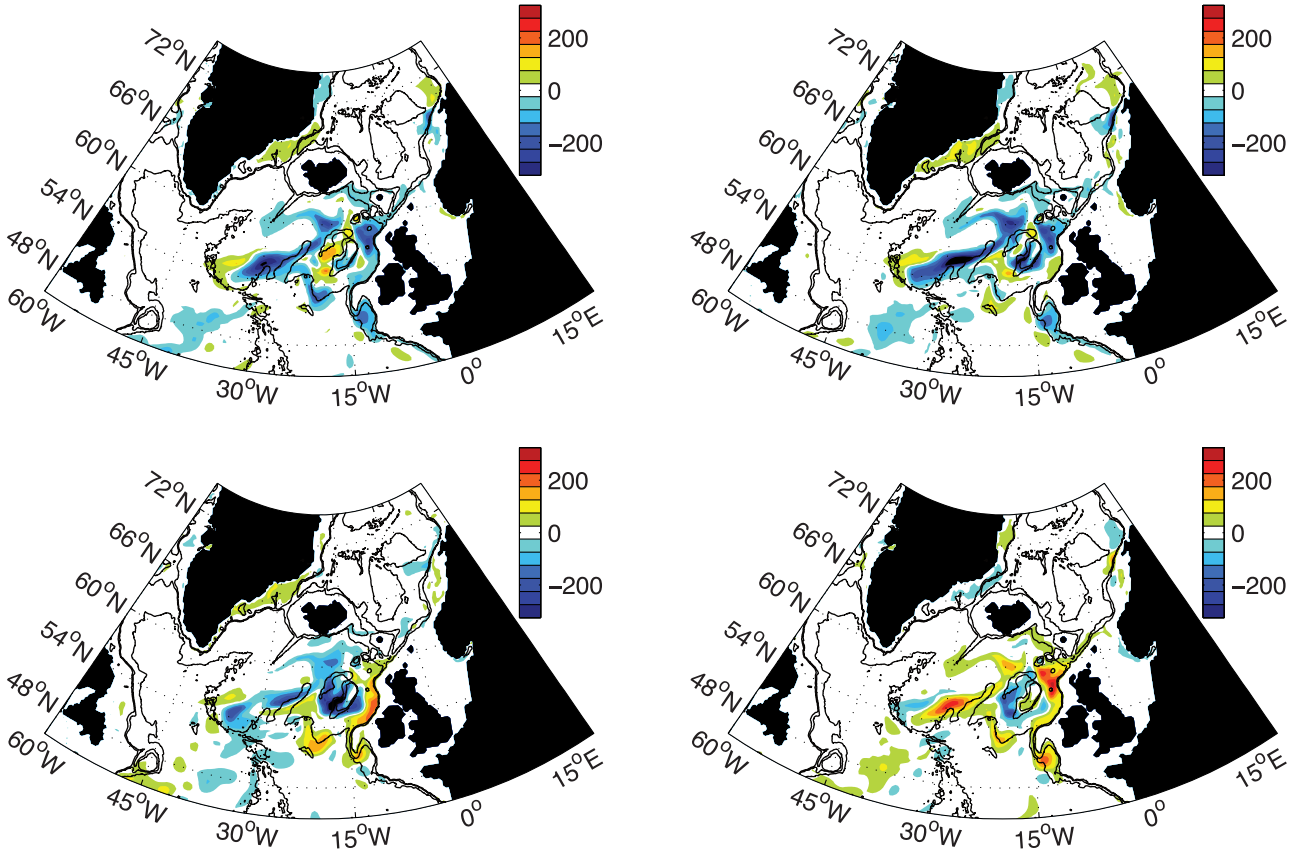

Figure 9. As in Figure 6 but for the period 1990–1995.

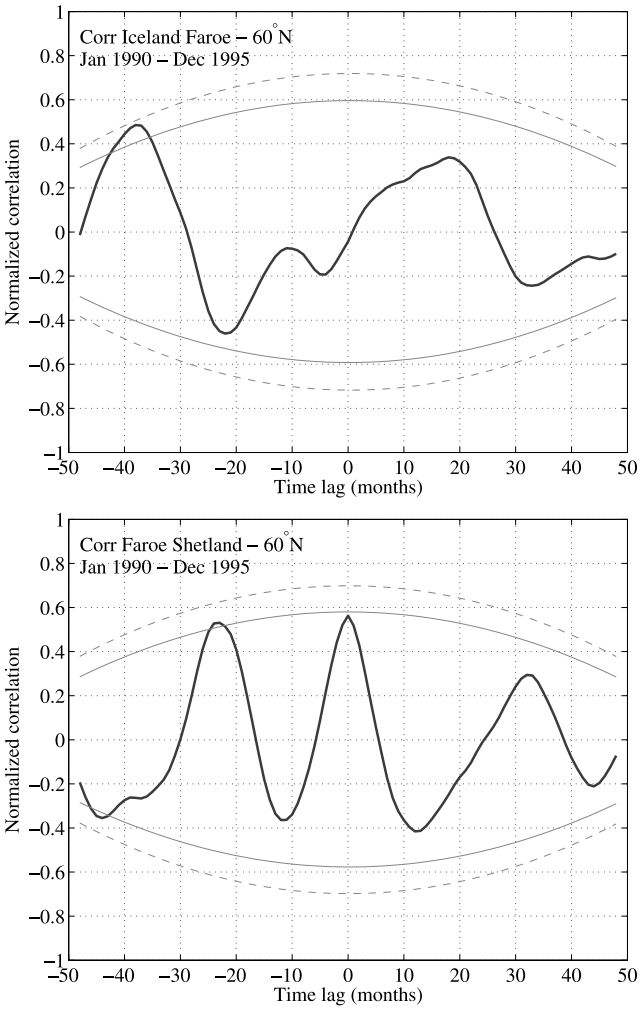

Figure 10. Correlation (top) between northward transports in the IF section 1990–1995 and the 60°N section, and (bottom) between the FS section and the 60°N section. Thin solid and dashed lines indicate respectively the 95 and 99% confidence intervals, estimated using a bootstrap algorithm with 10,000 permutations. Positive lag means that IF or FS is lagging the 60°N section.

vicinity of the Rockall Bank, compared to 1995–2001 when layer 12 was much thinner and layer 11 and partly layer 10 were filled instead.

4.5. Propagation of Signal Into the Nordic Seas

[32] To illustrate how a surface generated signal in mixed layer density is transferred into the deeper isopycnic layers, Hovmöller diagrams for layer thickness anomalies are shown for the section running from the North Atlantic into the Nordic Seas (Figure 15). The effect of the significant change in atmospheric forcing from 1995 to 1996 is clear. For the years 1993 to 1995 when the mixed layer became very dense, layer 11 was much thinner than normal and layer 12 much thicker, showing that the mixing reached the deepest of these layers in those years.

[33] Waters denser than those in layer 11 will only to a small extent pass over the GSR. It is thus to be expected that variations in water properties generated at the Rockall Bank,

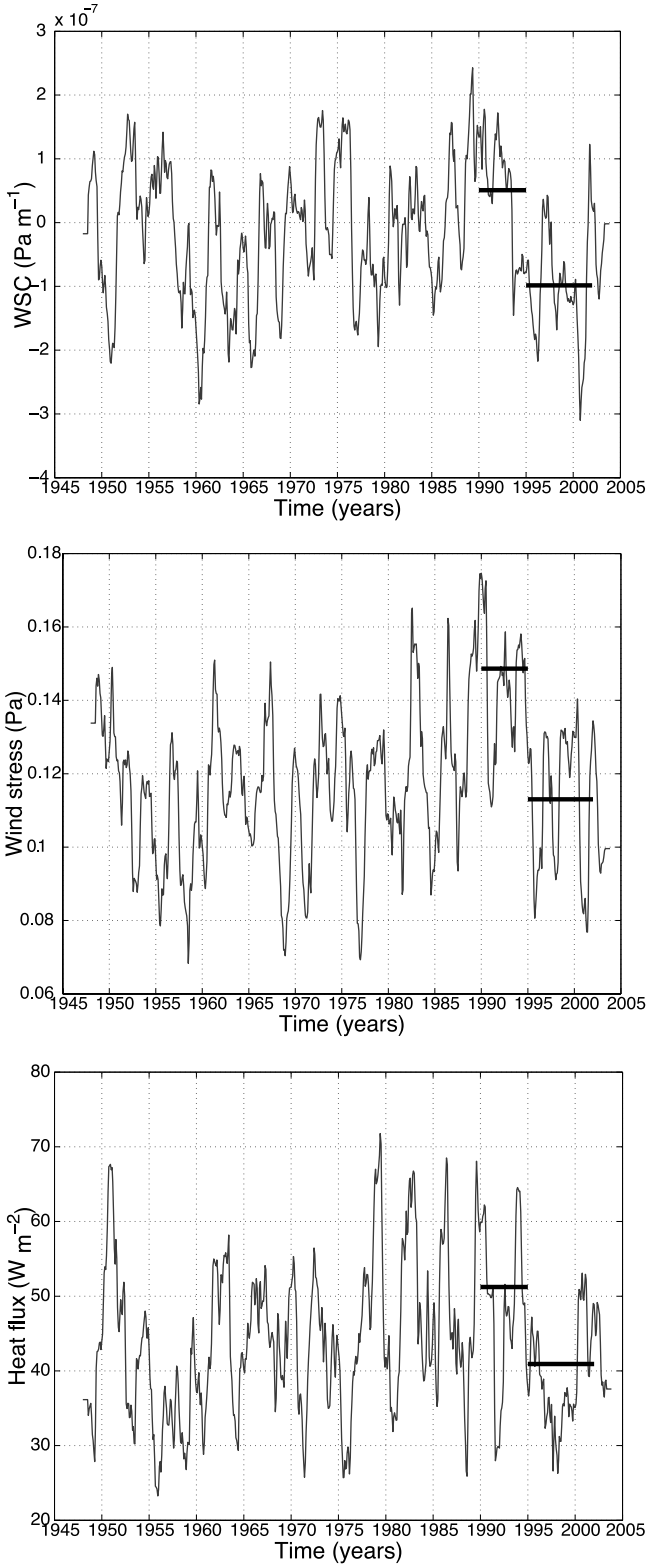

Figure 11. Time series of (top) WSC, (middle) wind stress, and (bottom) net heat loss over the Rockall Bank (20°W–10°W, 54°N–56°N) 1948–2003. The lines mark the averages for the periods discussed.

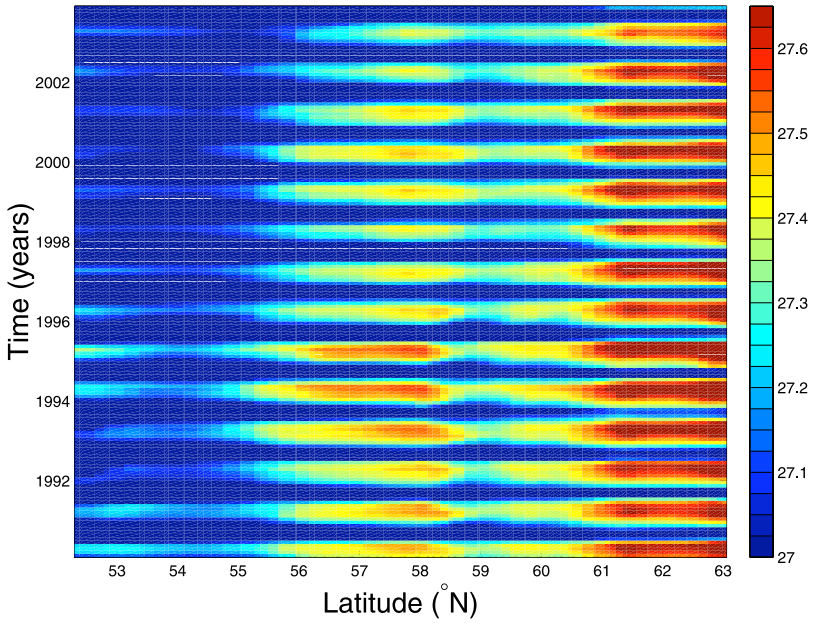

Figure 12. Hovmöller diagrams of mixed layer density (nondimensional σ_0 units) along the North Atlantic–Nordic Seas section at the Rockall Bank.

can only be transferred to the Nordic Seas if they are added to a layer that continues into the Nordic Seas. Variations in water mass properties below the sill depth will tend to follow f/H contours that do not enter the Nordic Seas, and therefore to less extent impact the flow north of the GSR. As shown by Figure 16, the main currents are deflected by the Rockall Bank and pass on the eastern side. In contrast, for the period 1995–2001, the thickness of layer 11 and the currents on the western flank are considerably increased.

5. Discussion

[34] The strength of the atmospheric forcing in the Rockall region turns out to be crucial for the relationships between the WSC at 55°N and the volume transports at Svinøy. The two periods in this study are therefore chosen to represent respectively weak and strong forcings.

[35] For the period with current meter observations (1995–2001), the atmospheric forcing over the northeastern parts of the North Atlantic was relatively weak (Figure 11), the mixed layer less dense (Figure 12), and the winter mixing only reached layer 11 causing a volume increase in this layer (Figure 16). A lag regression between volume transports over the Iceland-Faroe Ridge and the thickness of layer 11 (Figure 6), which is the densest layer crossing the GSR, indicates an expansion of this layer at the western flank of the Rockall Bank about one and a half year prior to inflow. With time the signal gradually strengthens toward the GSR before the flow over the Iceland-Faroe Ridge is enhanced. This chain of events suggests that the lag relationships between the WSC and the volume transports of Atlantic water into the Nordic Seas (Figure 4), is related to the wind mixing in the vicinity of the Rockall Bank.

[36] In contrast, the period prior to the start of the current meter observations (1990–1995) was characterized by very strong wind forcing over the northeastern North Atlantic (Figure 11), causing a much denser winter mixed layer during that period (Figure 12). As a result, the water produced during winter now feeds layer 12 during the spring restratification process, as evident in Figure 16. The water of layer 12 is in general too dense to be able to overcome the sill depths of the GSR, and the baroclinic signals are therefore not transmitted into the Nordic Seas. As a result, barotropic timescales will dominate the correlations between WSC and volume transports north of the ridge as indicated by Figure 8.

[37] The key result of this paper is that the communication of a baroclinic disturbance from the North Atlantic to the Nordic Seas is dependent upon which depth or isopycnic layer the signal is transferred to. This in turn depends on the strength of the atmospheric forcing, primarily during winters, and to which depth the vertical mixing reaches. The vertical mixing is seen to reach layers with greater density over banks and in shallow areas where enhanced bottom mixing makes the isopycnals dome. If the mixing goes down to a density layer which extends from the North Atlantic over the GSR to the Nordic Seas, the baroclinic signal can be transferred to the Nordic Seas. Alternatively, if the mixing goes deeper and generates a baroclinic signal in a density layer not reaching the Nordic Seas, the baroclinic signal will be deflected at the GSR and will to a less extent cause variations north of the ridge. The layers above layer 11 outcrop more frequently to the mixed layer, not only in the Rockall area, but also other places, while layer 11 is more exposed to the mixing at Rockall due to the topography. We believe that the reason for the strong regression between the inflow variability and the layer 11 thickness at Rockall with a time lag of 10–20 months is due to isolation of this layer from the mixed layer in the area between Rockall and GSR and further into the Nordic Seas. The layers above are more exposed to mixing in different areas and at different timescales, and will therefore cause vari-

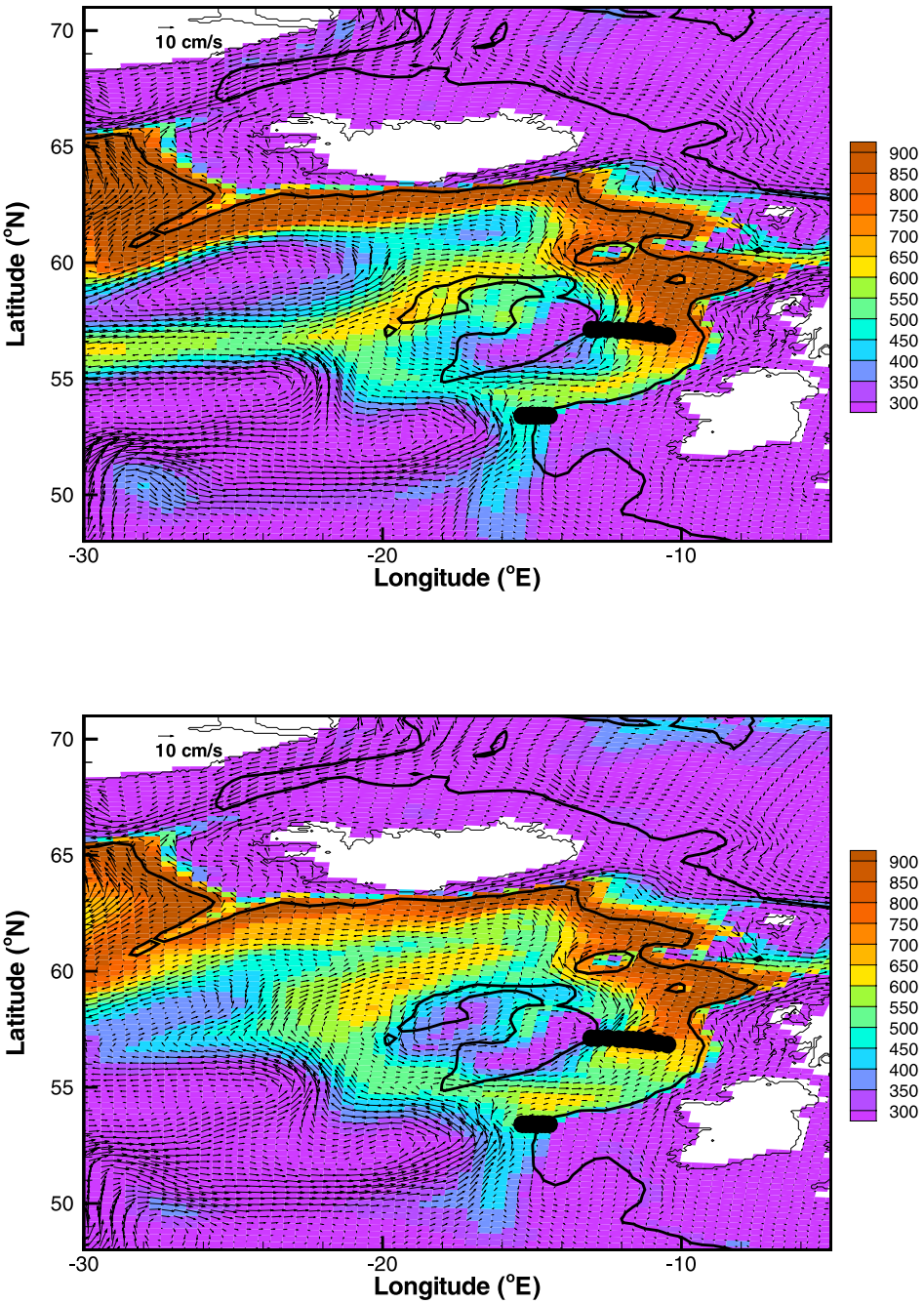

Figure 13. Simulated mixed layer depths and velocities in March (top) 1990–1995 and (bottom) 1996–2001. The sections indicated by rows of black circles in the plots mark the locations where observed and modeled density profiles shown in Figure 17 are taken. Black contour corresponds to 1000 m depth.

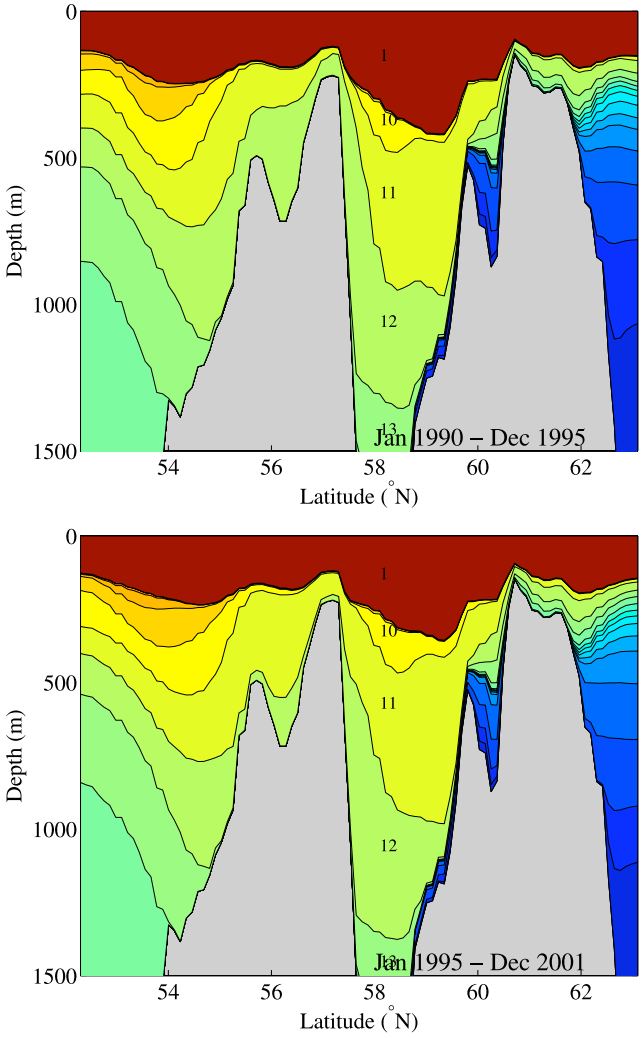

Figure 14. Vertical position of isopycnic layers along the North Atlantic–Nordic Seas section in (top) 1990–1995 and (bottom) 1995–2001.

ability in the inflow at different time lags with dependency on a greater range of areas.

[38] As manifested by the North Atlantic Oscillation index [*Hurrell et al.*, 2001], the atmosphere went from a period with very intense wintertime forcing to a record weak forcing from 1995 to 1996. Accompanying this shift, the subpolar gyre (SPG) has been shown to weaken (i.e., less eastward extension and less intense), and consequentially warmer and saltier water has entered the Nordic Seas [*Holliday*, 2003; *Hátun et al*, 2005b].

[39] The lag relationship between North Atlantic WSC and the Atlantic water inflow to the Nordic Seas, suggests a potential for predicting the inflow some 15 months ahead as found by *Orvik and Skagseth* [2003]. On the basis of our results, this relationship only exists for periods when the atmospheric forcing is relatively weak. For stronger forcing, as for the period 1990–1995, the wintertime mixing in the model reaches layers below the threshold depth of the GSR, and the baroclinic signals are propagating along the *f*/*H* contours not being communicated into the Nordic Seas. Interestingly, the observed relation between the WSC and the Svinøy transports breaks down after 2004 (K. A. Orvik, personal communication, 2006). This could, according to our interpretation, be related to the enhanced wintertime forcing in recent years, as seen in both the WSC and the heat fluxes (Figure 11). On the other hand, *Hátun et al.* [2005b] use the same model as in this study to show that there is a lag by 1 to 2 years between the time series for the salinity at Nordic Seas inflow and the time series for the SPG intensity. The potential of predicting volume transports along the Norwegian coast therefore seems less encouraging than for hydrographic quantities as shown by *Hátun et al.* [2005b]. Their mechanism seems to hold independent of forcing regime. The atmospheric forcing are probably the cause for the variability in both cases, but the mechanisms for generating the oceanic anomalies are different.

[40] Owing to limited amount of observational data, it is not trivial to assess the quality of the simulated mixed layer depth, a crucial parameter for the mechanism proposed in this study. However, a comparison between modeled and observed density profiles in the Rockall Trough, east of the Rockall Bank (Figure 17), does indicate that the model reasonably captures the nature. This can be argued in terms of the depth of the thermoclines, and the shape and the range of the density profiles.

[41] It should also be noted that the results presented above partly depends on short time series with inherent autocorrelations, making it a challenge to assess the significance of the results. We have therefore been careful not to put too much emphasize on details, and instead focused on the difference between the period with weak atmospheric forcing used by *Orvik and Skagseth* [2003], and the period prior to this with much stronger forcing. The large differences in mixed layer density, internal density structure, and statistical properties of the two periods, make us confident that the main conclusions are trustworthy.

6. Summary and Concluding Remarks

[42] The aim of this study has been to investigate how baroclinic processes south of the GSR may influence the variability in the inflow of Atlantic water to the Nordic Seas, and to determine the degree of predictability in the system. A motivation has been the results of *Orvik and Skagseth* [2003], which indicated that the North Atlantic WSC was leading the Atlantic water transport along the Norwegian Coast by 15 months. Since variations in the northward flux of salt and temperature in this region to a large extent is controlled by the volume flux on interannual timescales [*Orvik and Skagseth*, 2005; *Mauritzen et al.*, 2006], this would mean that also the fluxes of heat and salt, and thereby the hydrographical conditions important for biomass production and fish stock distribution, could be predicted.

[43] In accordance with observations, model results in this study show that the volume transport at Svinøy, off the west coast of Norway, correlates with the zonally averaged (40°W–10°E) WSC at 55°N in the North Atlantic for the period 1995–2001, with an approximate time lag of 15 months. In our model this is related to the mixing depth in the vicinity of the Rockall Bank. In periods of modest atmospheric forcing, as for 1995–2001, the mixing is

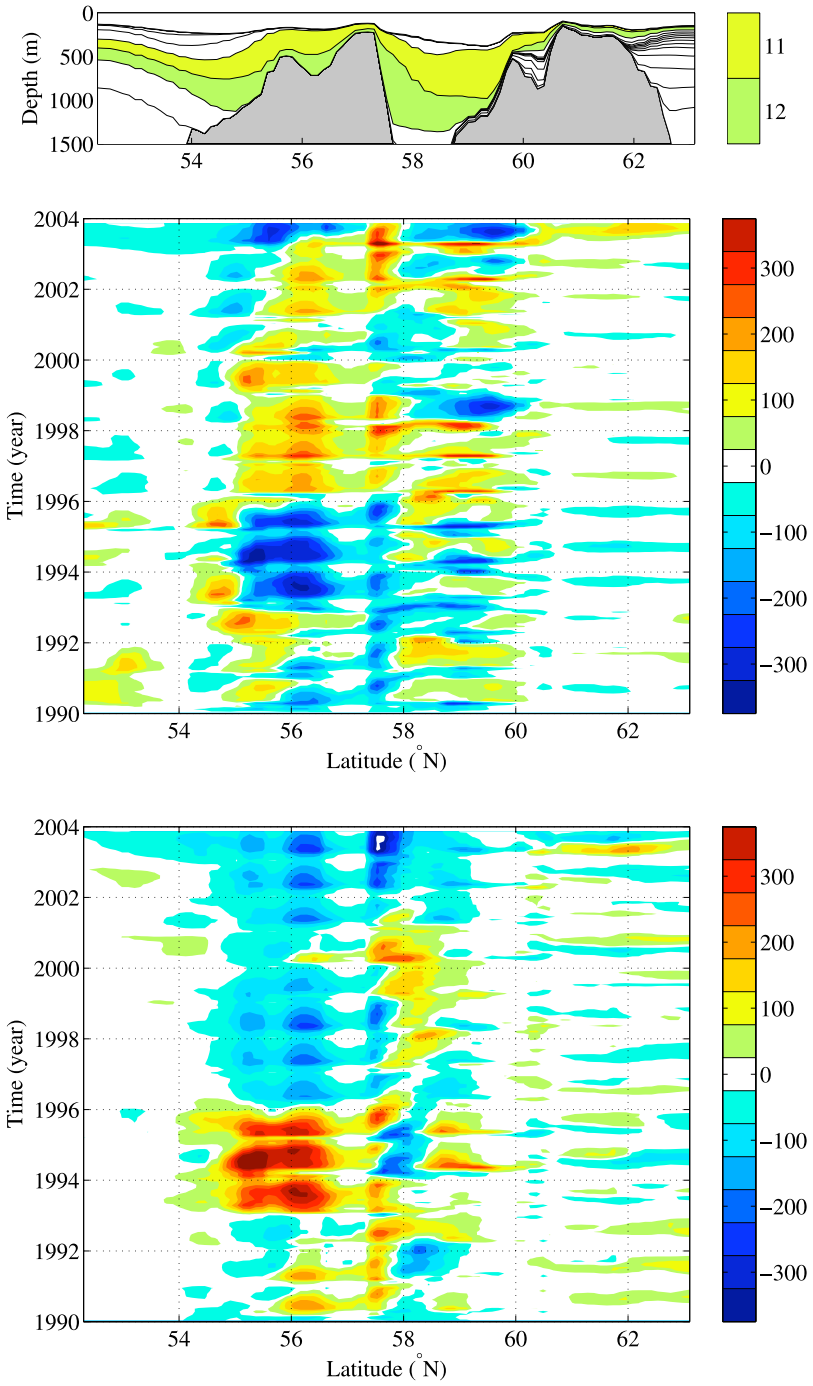

Figure 15. (top) Vertical section, and Hovmöller diagrams of anomalous layer thicknesses along the North Atlantic–Nordic Seas section at the Rockall Bank for layers (middle) 11 and (bottom) 12.

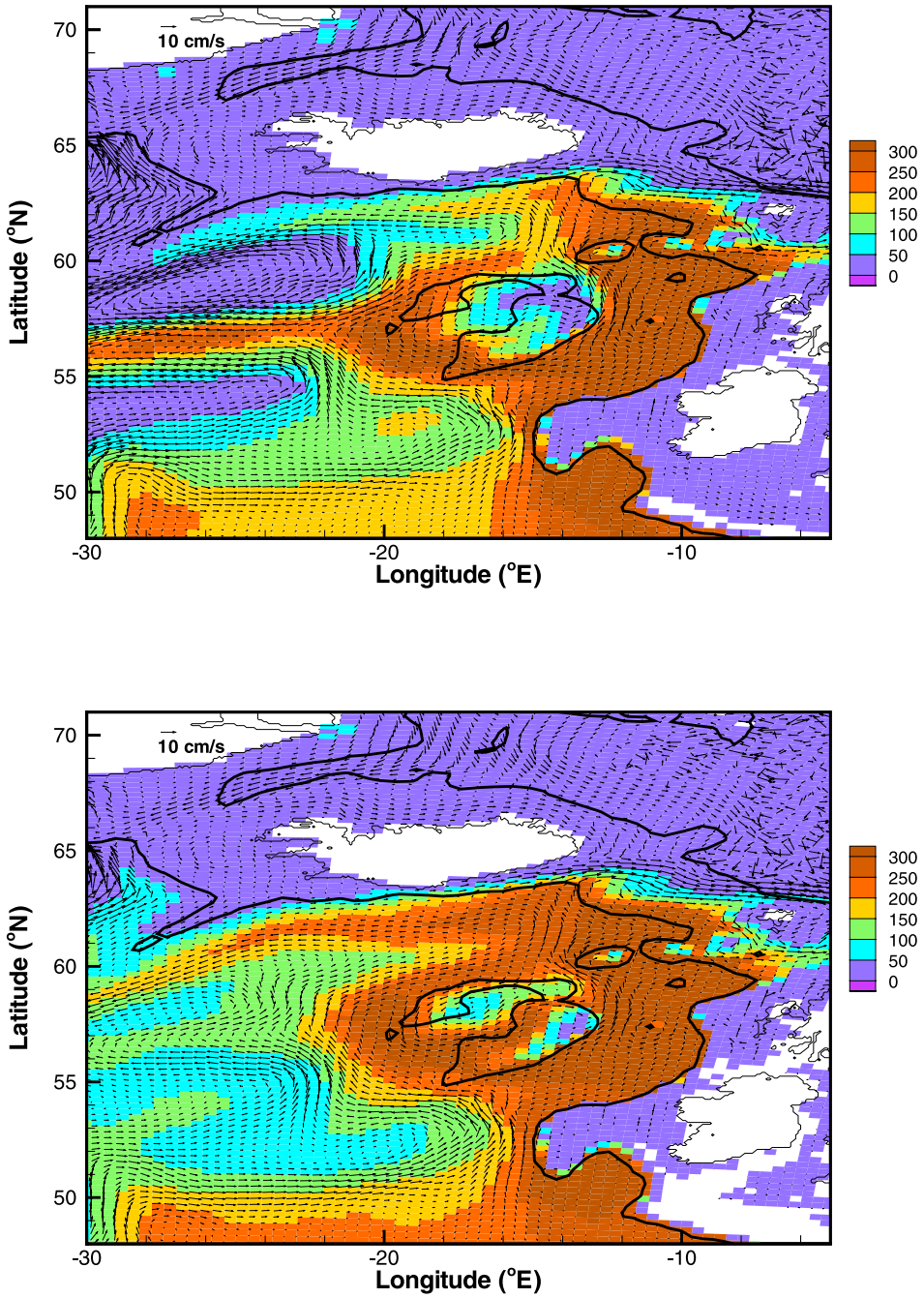

Figure 16. Thickness and horizontal velocities of layer 11 around the Rockall Bank in (top) 1990–1995 and (bottom) 1995–2001. Black contour corresponds to 1000 m depth.

relatively shallow and reaches an isopycnic layer that extends into the Nordic Seas. For these years, variations in the atmospheric forcing and thus the mixing strength are transmitted into the Nordic Seas, and a predictability based on baroclinic adjustment timescales is suggested. On the other hand, for periods of intense atmospheric forcing and deeper mixing, any signal that is generated by a WSC anomaly will be transferred to the deeper layers, following f/H contours that do not extend into the Nordic Seas. Thus the potential for predictability seems to vanish for strong forcing regimes.

[44] It should be emphasized that the results shown here do not exclude the importance of other processes than those discussed, which in many periods may have even stronger influence on the transport variability. We have nevertheless pointed to one mechanism that may be of great importance with respect to the potential for prediction, namely the wintertime ventilation depth south of the GSR and in particular in the vicinity of the Rockall Bank. Regression of isopycnic layer thickness on transport variability clearly points toward this region as being a "hot spot" for inflow variability.

[45] Although it has not been possible to find relations between the WSC and downstream volume fluxes that hold independent of time, we have here presented results that give more insight into the processes involved. Further

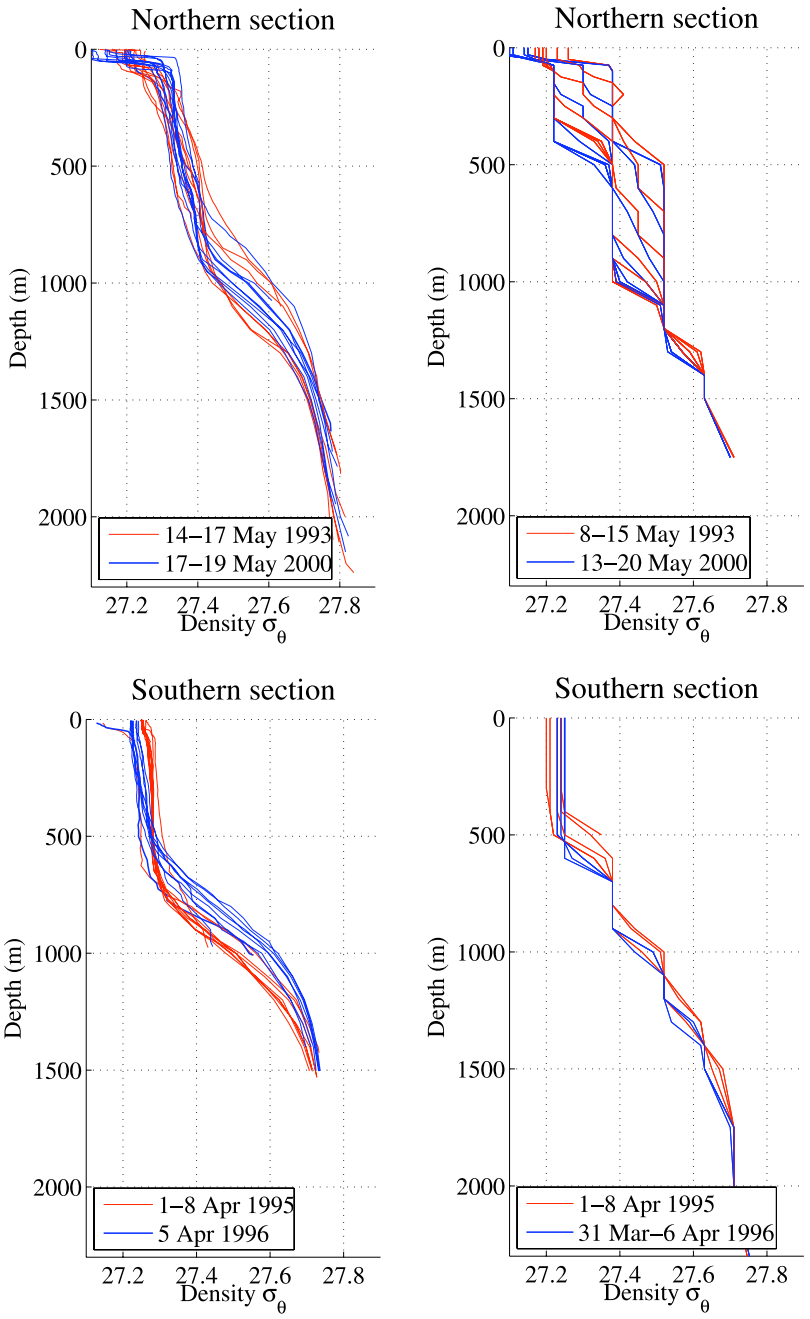

Figure 17. (left) Observed and (right) modeled density profiles from the two sections in the Rockall Trough indicated in the Figure 13. Red curves are from spring 1993 (top plots) and 1995 (bottom plots), and blue curves from 2000 (top plots) and 1996 (bottom plots). The modeled sections are weekly averages from the same weeks as the observations are taken, and the variables are interpolated from the isopycnal layers onto Levitus depths. The observational data are from the NISE database [*Nilsen et al.*, 2007].

analyses of atmospheric forcing fields and oceanic transports in higher-resolution model experiments should be performed in order to carry out more detailed predictability analyses in the years to come.

[46] **Acknowledgments.** We thank Tor Eldevik and two anonymous reviewers for helpful comments on the manuscript. This work was supported by the Nordic Council of Ministers through a 5-year fellowship related to the West Nordic Ocean Climate Programme, by the Norwegian Research Council projects NOClim, NorClim, and Pocahontas and by the Norwegian Supercomputer Committee through a grant of computing time. This is publication A188 from the Bjerknes Centre for Climate Research.

References

Bentsen, M., and H. Drange (2000), Parameterizing surface fluxes in ocean models using the NCEP/NCAR reanalysis data, in *Regional Climate Development Under Global Warming, RegClim Gen. Tech. Rep.* 4, pp. 149–158, Norw. Inst. for Air Res., Kjeller, Norway.

Bentsen, M., H. Drange, T. Furevik, and T. Zhou (2004), Simulated variability of the Atlantic meridional overturning circulation, *Clim. Dyn.*, *22*, 701–720.

Bleck, R., C. Rooth, D. Hu, and L. T. Smith (1992), Salinity-driven thermocline transients in a wind- and thermohaline-forced isopycnic coordinate model of the North Atlantic, *J. Phys. Oceanogr.*, *22*, 1486–1505.

Collins, M., et al. (2006), Interannual to decadal climate predictability in the North Atlantic: A multimodel-ensemble, *J. Clim.*, 1195–1203.

Drange, H., and K. Simonsen (1996), Formulation of air-sea fluxes in the ESOP2 version of MICOM, *Rep. 125*, Nansen Environ. and Remote Sens. Cent., Bergen, Norway.

Drange, H., R. Gerdes, Y. Gao, M. Karcher, F. Kauker, and M. Bentsen (2005), Ocean general circulation modelling of the Nordic Seas, in *The Nordic Seas: An Integrated Perspective*, *Geophys. Monogr. Ser.*, vol. 158, edited by H. Drange et al., pp. 199–219, AGU, Washington, D.C.

Eldevik, T., F. Straneo, A. B. Sandø, and T. Furevik (2005), Pathways and export of Greenland Sea Water, in *The Nordic Seas: An Integrated Perspective*, *Geophys. Monogr. Ser.*, vol. 158, edited by H. Drange et al., pp. 89–103, AGU, Washington, D.C.

Fairall, C. W., E. F. Bradley, D. P. Rogers, J. B. Edson, and G. S. Young (1996), Bulk parameterization of air-sea fluxes for Tropical Ocean–Global Atmosphere Coupled-Ocean Atmosphere Response Experiment, *J. Geophys. Res.*, *101*, 3747–3764.

Furevik, T. (2001), Annual and interannual variability of Atlantic Water temperatures in the Norwegian and Barents Seas: 1980–1996, *Deep Sea Res., Part I*, *48*, 383–404.

Furevik, T., and J. E. Ø. Nilsen (2005), Large-scale atmospheric circulation variability and its impacts on the Nordic Seas ocean climate, in *The Nordic Seas: An Integrated Perspective*, *Geophys. Monogr. Ser.*, vol. 158, edited by H. Drange et al., pp. 105–136, AGU, Washington, D.C.

Furevik, T., M. Bentsen, H. Drange, J. Johannessen, and A. Korablev (2002), Temporal and spatial variability of the sea surface salinity in the Nordic Seas, *J. Geophys. Res.*, *107*(C12), 8009, doi:10.1029/2001JC001118.

Gill, A. E. (1982), *Atmosphere–Ocean Dynamics*, Academic Press, London.

Hansen, B., and S. Østerhus (2000), North Atlantic–Nordic Seas exchanges, *Prog. Oceanogr.*, *45*, 109–208.

Harder, M. (1996), Dynamik, rauhigkeit und alter des meereises in der arktis, *Ph.D. thesis*, Alfred-Wegener-Inst. fur Polar- und Meeresforsch., Bremerhaven, Germany.

Hátun, H., A. B. Sandø, H. Drange, and M. Bentsen (2005a), Seasonal to decadal temperature variations in the Faroe-Shetland inflow waters, in *The Nordic Seas: An Integrated Perspective*, *Geophys. Monogr. Ser.*, vol. 158, edited by H. Drange et al., pp. 239–238, AGU, Washington, D.C.

Hátun, H., A. B. Sandø, H. Drange, B. Hansen, and H. Valdimarsson (2005b), Influence of the Atlantic Subpolar Gyre on the thermohaline circulation, *Science*, *309*, 1841–1844.

Helland-Hansen, B., and F. Nansen (1909), Report on Norwegian fish and marine investigations, in *The Norwegian Sea*, *Rep., Norw. Fish. Mar. Invest.*, 2, 359 pp.

Hibler, W. D., III (1979), A dynamic thermodynamic sea ice model, *J. Phys. Oceanogr.*, *9*, 815–846.

Holliday, N. P. (2003), Air-sea interaction and circulation changes in the northeast Atlantic, *J. Geophys. Res.*, *108*(C8), 3259, doi:10.1029/2002JC001344.

Hurrell, J. W., Y. Kushnir, and M. Visbeck (2001), The North Atlantic Oscillation, *Science*, *291*, 603–605.

Kistler, R., et al. (2001), The NCEP-NCAR 50-year reanalysis: Monthly means CD-ROM and documentation, *Bull. Am. Meteorol. Soc.*, 247–268.

Lehodey, P., et al. (2006), Climate variability, fish and fisheries, *J. Clim.*, *19*, 5009–5020.

Levitus, S., and T. P. Boyer (1994), *World Ocean Atlas 1994*, vol. 4, Temperature, NOAA Atlas NESDIS 4, NOAA, Silver Spring, Md.

Levitus, S., R. Burgett, and T. P. Boyer (1994), *World Ocean Atlas 1994*, vol. 3, Salinity, NOAA Atlas NESDIS 3, NOAA, Silver Spring, Md.

Mauritzen, C., S. S. Hjøllo, and A. B. Sandø (2006), Passive tracers and active dynamics—A model study of hydrography and circulation in the northern North Atlantic, *J. Geophys. Res.*, *111*, C08014, doi:10.1029/2005JC003252.

Nilsen, J. E. Ø., Y. Gao, H. Drange, T. Furevik, and M. Bentsen (2003), Simulated North Atlantic Seas water mass exchanges in an isopycnic coordiante OGCM, *Geophys. Res. Lett.*, *30*(10), 1536, doi:10.1029/2002GL016597.

Nilsen, J. E. Ø., H. Hátun, K. A. Mork, and H. Valdimarsson (2007), The NISE data collection, technical report, Faroese Fish. Lab.,Torshavn, Faroe Islands.

Oki, T., and Y. C. Sud (1998), Design of Total Runoff Integrating Pathways (TRIP)—A global river channel network, *Earth Interact.*, *2*, 1–37.

Orvik, K. A., and P. Niiler (2002), Major pathways of Atlantic water in the northern North Atlantic and Nordic Seas toward Arctic, *Geophys. Res. Lett.*, *29*(19), 1896, doi:10.1029/2002GL015002.

Orvik, K. A., and Ø. Skagseth (2003), The impact of the wind stress curl in the North Atlantic on the Atlantic inflow to the Norwegian Sea toward the Arctic, *Geophys. Res. Lett.*, *30*(17), 1884, doi:10.1029/2003GL017932.

Orvik, K. A., and Ø. Skagseth (2005), Heat flux variations in the eastern Norwegian Atlantic current toward the Arctic from moored instruments, 1995–2005 current, *Geophys. Res. Lett.*, *32*, L14610, doi:10.1029/2005GL023487.

Orvik, K. A., Ø. Skagseth, and M. Mork (2001), Atlantic inflow to the Nordic Seas: current structure and volume fluxes from moored current meters, VM-ADCP and SeaSoar-CTD observations, 1995–1999, *Deep Sea Res., Part I*, *48*, 937–957.

Østerhus, S., W. R. Turrell, S. Jónsson, and B. Hansen (2005), Measured volume, heat, and salt fluxes from the Atlantic to the Arctic Mediterranean, *Geophys. Res. Lett.*, *32*, L07603, doi:10.1029/2004GL022188.

Sandø, A. B., and H. Drange (2006), A nested model of the Nordic Seas, *Tech. Rep. 268*, Nansen Environ. and Remote Sens Cent., Bergen, Norway.

Zoubir, A. M., and B. Boashash (1998), The bootstrap and its application in signal processing, *IEEE Signal Process. Mag.*, *15*, 55–76.

T. Furevik, Geophysical Institute, University of Bergen, Allegt 70, N-5007 Bergen, Norway.

A. B. Sandø, G. C. Rieber Climate Institute, Nansen Environmental and Remote Sensing Center, Thormøhlensgate 47, N-5006 Bergen, Norway. (anne.britt.sando@nersc.no)